

Journal of Materials Chemistry C

Accepted Manuscript



This is an *Accepted Manuscript*, which has been through the Royal Society of Chemistry peer review process and has been accepted for publication.

Accepted Manuscripts are published online shortly after acceptance, before technical editing, formatting and proof reading. Using this free service, authors can make their results available to the community, in citable form, before we publish the edited article. We will replace this *Accepted Manuscript* with the edited and formatted *Advance Article* as soon as it is available.

You can find more information about *Accepted Manuscripts* in the [Information for Authors](#).

Please note that technical editing may introduce minor changes to the text and/or graphics, which may alter content. The journal's standard [Terms & Conditions](#) and the [Ethical guidelines](#) still apply. In no event shall the Royal Society of Chemistry be held responsible for any errors or omissions in this *Accepted Manuscript* or any consequences arising from the use of any information it contains.

ARTICLE

Efficient Organic-Inorganic Hybrid Hole Injection Layer for Organic Light-Emitting Diodes by Aqueous Solution Doping

Cite this: DOI:
10.1039/x0xx00000x

Received 00th January 2012,
Accepted 00th January 2012

DOI: 10.1039/x0xx00000x

www.rsc.org/

Ya-Li Deng, Yue-Min Xie, Lei Zhang, Zhao-Kui Wang,* and Liang-Sheng Liao*

The authors develop an aqueous solution-processed hole injection layer, MoO₃ doped copper phthalocyanine-3,4,4',4'' tetra-sulfonated acid tetra sodium salt (TS-CuPc), in organic light-emitting diodes (OLEDs) via an environmentally-friendly and easy fabricating process. The generation of charge transfer complex in TS-CuPc:MoO₃ composite films are confirmed by absorption spectra and the X-ray photoemission spectroscopy (XPS) measurements. Enhanced hole injection in OLEDs is attributed to the decreased hole barrier at the ITO side, which is agreed with the Schottky thermal emission evaluation. The efficient modifications of ITO by TS-CuPc:MoO₃ is further confirmed by the ultraviolet photoemission spectroscopy (UPS) measurements.

Introduction

Organic light-emitting diodes (OLEDs) have been regarded as one of the most promising technologies for next generation solid-state lighting and displays.¹ Increasing carrier injection from the electrodes in to the emitting layer is generally required for fabricating high efficiency OLEDs.²⁻⁴ There exists a large offset of energy levels between the work function of commonly used indium tin oxide (ITO) and the highest occupied molecular orbital (HOMO) of commonly used hole-transporting layers (HTLs).⁵⁻⁶ Many methods, such as ultraviolet (UV)-ozone and/or CF_x treatment,⁷⁻⁸ thermal annealing,⁹ self-assembling¹⁰⁻¹¹, and inserting a thin hole injection layer (HIL), have been developed to optimize the hole injection at the anode side. Transition metal oxides based inorganic materials,¹² such as molybdenum oxide (MoO₃),¹³ vanadium oxide (V₂O₅),¹⁴ tungsten oxide (WO₃)¹⁵ and nickel oxide (NiO)¹⁶ have been widely used in OLEDs to reduce the hole injection barrier. In particular, aqueous solution-processed MoO₃ has been reported recently as an effective anode interfacial layer in OLEDs with comparable efficiency and reduced driving voltage.¹⁷⁻¹⁹ Copper phthalocyanine (CuPc) is also a commonly used hole injection material in OLEDs to improve the device efficiency.²⁰ However, an insertion of a CuPc layer often leads to substantial increase in the driving voltage of the OLEDs.²¹ Recently, Bechara *et al.* reported that the copper phthalocyanine-3,4,4',4'' tetra-

sulfonated acid tetra sodium salt (TS-CuPc) can also be used as hole interfacial layer in organic solar cells.²² Different from the CuPc, TS-CuPc is an excellent aqueous solution-processed material which allows high dissolving concentration in water.²³ Electrical doping in organic materials is very efficient for resolving the issues of low conductivity and high carrier barriers in organic electronics. In particular, transition metal oxides (*i.e.*, MoO₃) doped organic semiconductor demonstrated special merits on improving the device performance.^{4,24-25} Both TS-CuPc and MoO₃ can dissolve into the water to a certain extent. Therefore, a doping hole interfacial layer can be formed by mixing TS-CuPc and MoO₃ in aqueous solutions.

In this work, we introduce MoO₃ doped TS-CuPc as a hole injection and transport material in OLEDs based on aqueous solution processing. Electrical doping with efficient charge transfer is realized in the aqueous solutions. The devices with the newly developed hole interfacial layer demonstrate not only improved power efficiency but also significantly reduced operation voltage. Unlike other dopants, the doping ratio of MoO₃ allows higher than 50 percent without blocking hole transporting characteristics in OLEDs. In addition, the aqueous solution-processed doping technique is very simple and environment-friendly by dissolving commercial MoO₃ and TS-CuPc into the deionized water simultaneously without any toxicity.

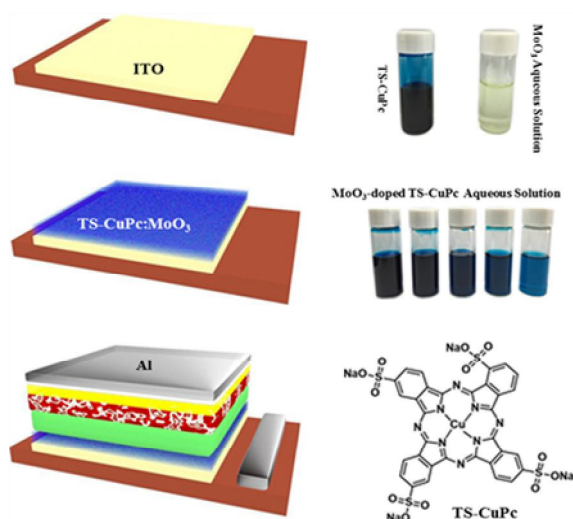


Fig. 1 A schematic diagram of device structure of TS-CuPc:MoO₃ based OLEDs and the chemical structure of the TS-CuPc molecule.

Experimental

Materials and Devices Fabrication.

MoO₃ and TS-CuPc aqueous solutions were firstly prepared by dissolving them, respectively, into the deionized water with over 10 hrs stirring in air at room temperature. Additional heating (70 °C) and prolonged stirring time are required for MoO₃ if the concentration is higher than 1 wt%. The prepared MoO₃ and TS-CuPc aqueous solutions were then blended together with concentrations of 2 mg/ml with different volume ratios. 4,4',4''-tris(N-carbazolyl)-triphenylamine (TCTA) is used as both the hole transporting layer and the host material, Iridium(III)bis(2-methylidibenzo [f,h]quinoxaline)(acetylacetonate) (Ir(MDQ)₂acac) as the red phosphorescent dopant, 1,3,5-tri[(3-pyridyl)-phen-3-yl]benzene (TmPyPB) as the electron transporting material, 8-hydroxyquinolino lithium (Liq) as the electron injecting material, and aluminum (Al) as the cathode. All the materials have the purity higher than 99% and are used without further purification.

OLEDs are fabricated in ITO-coated glass substrate with thickness of ~110 nm and a sheet resistance of 15 Ω/square. The substrate was pre-patterned by photolithography to give an effective device area of 9 mm². Prior to device fabrication, the substrates were thoroughly cleaned in sequential ultrasonic baths of detergent, acetone, isopropanol, and deionized water. After ultraviolet ozone treatment for 15 min, TS-CuPc:MoO₃ interfacial layer was spin-coated onto the ITO substrate followed by baking at 140°C in air for 15 min. And then, the substrates were transferred into a high-vacuum system at a base pressure of 10⁻⁶ Torr for depositing the organic and metal layers. The device has a structure of ITO/TS-CuPc:MoO₃ (5.5 nm)/TCTA (45 nm)/TCTA:Ir(MDQ)₂acac 4 wt% (15 nm)/TmPyPB (40 nm)/Liq (2 nm)/Al (120 nm). Fig. 1 shows a

schematic diagram of the device structure and the chemical structure of the TS-CuPc.

Devices Characterization.

The electroluminescence (EL) characteristics are measured using a constant current source (Keithley 2400 SourceMeter) with a photometer (Photo Research SpectraScan PR 655). X-ray photoemission spectroscopy (XPS) analysis was obtained using a Kratos AXIS UltraDLD ultrahigh vacuum (UHV) surface analysis system with a monochromatic aluminum K_α source (1486.6 eV). Ultraviolet photoemission spectroscopy (UPS) analysis was carried out with an unfiltered He I (21.2 eV) gas discharge lamp and a hemispherical analyzer. All measurements were carried out at room temperature under ultrahigh vacuum. The photoelectrons are collected by a hemispherical analyzer with a total instrumental energy resolution of 0.1 eV for the UPS measurements and 0.5 eV for the XPS measurements. In all UPS and XPS spectra, the Fermi level (E_F) is referred as the zero binding energy. The absorption spectra were measured with an UV/Vis spectrophotometer (PerkinElmer Lambda 750). Atomic force microscopy (AFM) images of the interfacial films were obtained using a Veeco Multimode V instrument. The temperature dependence of current density-voltage (J - V) characteristics were characterized in a cryogenic probe station (Lake Shore, CRX-4K) connected to a Keithley 4200-SCS semiconductor parameter analyzer in N₂ environment.

Results and discussion

MoO₃ doped TS-CuPc Interfacial Films

Atomic force microscopy (AFM) evaluation (Supporting Information) revealed that there were no noticeable differences in root-mean-square (RMS) values among the MoO₃ doped TS-CuPc films with different doping concentrations (10%, 30%, 70%, and 90%). Fig. 2 shows the AFM surface image of TS-CuPc, MoO₃, and MoO₃ (30%) doped TS-CuPc films with RMS of 2.83 nm, 2.77 nm, and 2.44 nm, respectively. By MoO₃ doping, the roughness of TS-CuPc:MoO₃ composite film was slightly lowered compared to the pristine TS-CuPc film. This means that the aqueous solution doping can provide a smooth interfacial layer, which is beneficial for device performance and stability.

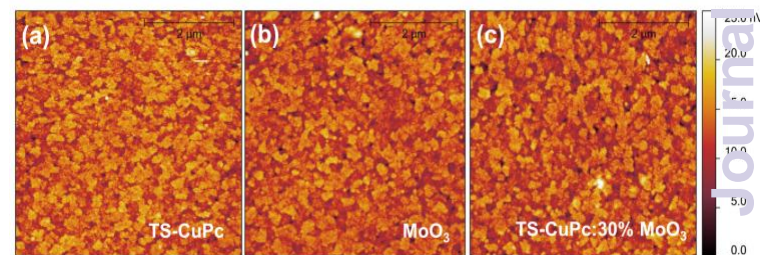


Fig. 2 AFM surface image of TS-CuPc, MoO₃, and MoO₃ (30%) doped TS-CuPc films.

Fig. 3 shows the UV/Vis absorption spectra of TS-CuPc, and MoO₃ (30%) doped TS-CuPc films. Additional absorption peak (1425 nm) appeared in the near-infrared (NIR) region suggests the efficient formation of the charge transfer complex (CTC) between MoO₃ and TS-CuPc. Past studies mainly focused on the P^{δ+}-N^{δ-} type CTC,²⁶⁻²⁸ which means that the p-type semiconductors donate electrons to the n-type semiconductors during the doping process.²⁹ The intensity of the additional peaks generally depends on the doping concentration of the N-type materials. Recently, another opposite charge-transfer condition (P^{δ+}-N^{δ+}), corresponding to the electron transfer (n-type material donating electrons to p-type material), was reported.³⁰ In this condition, both p-type and n-type molecules require low- and high-lying Fermi levels, which is similar as the exciplex emission reported recently by Ng *et al.*³¹ The energy gap in this kind of emission is always less than the difference between the highest occupied molecular orbital (HOMO) and lowest unoccupied molecular orbital (LUMO) levels of individual constituting molecules. The peak intensity 1425 nm seems to have nothing to do with the MoO₃ doping concentration (Supporting Information). The invariable intensity of the additional peak in NIR region is assumed to be related to the exciplex formation. In the visible region, two strong absorption peaks of TS-CuPc experienced a shift to a shorter wavelength as the MoO₃ doping concentration was increased (Supporting Information). Particularly, the left characteristic peak of TS-CuPc decreased due to the dilution of TS-CuPc aqueous solution with aqueous MoO₃ solution. This indicates that the transition energy from π*-orbital to π-orbital as the MoO₃ donates electrons to the TS-CuPc is decrescent,^{32, 33} resulting in the blue shift of the UV-visible spectra. This can also explain why the red device showed better performance to some extent since the emission peak of Ir(MDQ)₂acac is about 600 nm.

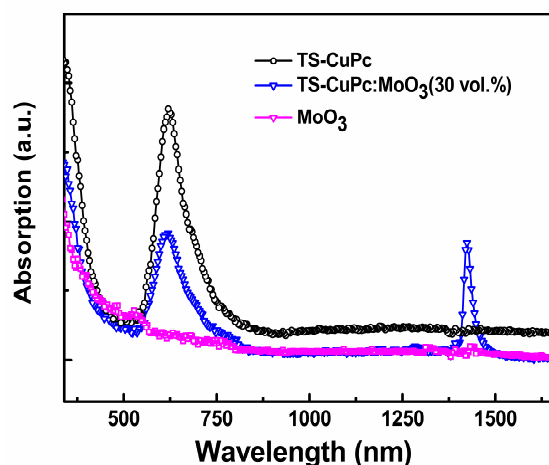


Fig. 3 UV/Vis absorption spectra of TS-CuPc, MoO₃ and MoO₃ (30%) doped TS-CuPc films.

To better understand the underlying mechanism of charge transfer complex in TS-CuPc:MoO₃ composite films, XPS

analysis is carried out as shown in Fig. 4. Compared with pristine MoO₃ film, the peak of Mo 3d in TS-CuPc:MoO₃ composite film shifts slightly to the higher binding energy. By MoO₃ doping, the N 1s peak in TS-CuPc is broadened, C 1s and O 1s shift slightly to the low binding energy. It indicates that TS-CuPc and MoO₃ showed a negligible charge transfer with a flat energy-band structure sharing common vacuum levels (VLs) before interacting with each other. When combining them into one layer by doping, MoO₃ donates the electrons to TS-CuPc, giving rise to partial CTC.^{34,35} And the long-wavelength optical absorption band in NIR region was also attributed to the CTC formation, which exhibits a promising application in NIR photovoltaic devices.

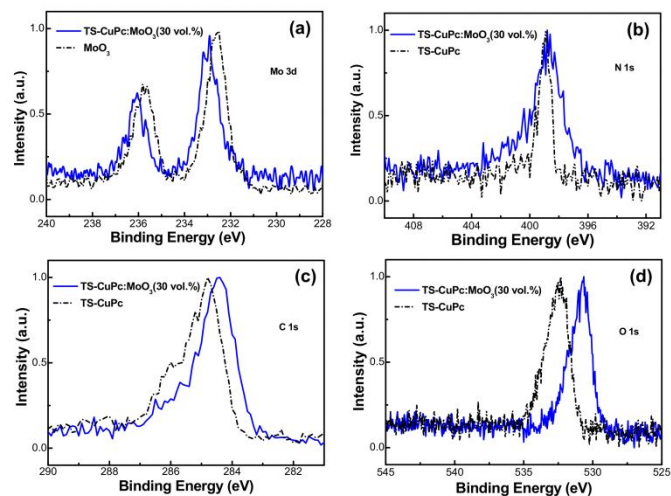


Fig. 4 XPS core-level spectra of (a) Mo 3d of MoO₃ and TS-CuPc:MoO₃ (30%) films; (b) N 1s, (c) C 1s and (d) O 1s of TS-CuPc and TS-CuPc:MoO₃ (30%) films.

TS-CuPc: MoO₃ Interfacial Layer Based OLEDs

A group of TS-CuPc:MoO₃ interfacial layer based OLEDs with different doping concentration were fabricated. Fig. 5 (a) shows the *J-V* characteristics dependent on the MoO₃ doping concentration. Obviously, the driving voltage presents a significant decrease with the increase of the MoO₃ ratio. The pristine MoO₃ based device (100% MoO₃ doping) shows the lowest driving voltage. Instead, pristine TS-CuPc based device shows the highest driving voltage due to the easy crystallization of TS-CuPc. It means that the crystallization of TS-CuPc film could be suppressed by MoO₃ doping, which will improve the device performance in some extent. Fig. 5 (b) shows the current efficiency and power efficiency characteristics in TS-CuPc, MoO₃ and MoO₃ doped TS-CuPc (30%) interfacial layer based OLEDs. The performance of the devices without any hole interfacial layer and with PEDOT:PSS as interfacial layer are also shown for comparison. The detailed device performance is summarized in the Table 1. The device with MoO₃ doped TS-CuPc interfacial layer exhibits the highest current efficiency and power efficiency of 42 cd/A and 40.1 lm/W, respectively. Specifically, over 65% enhancement in power efficiency is

achieved compared to the device without any interfacial modification. The pristine TS-CuPc based device shows the lowest power efficiency because of the highest driving voltage as shown in Fig. 5 (a). Noticeably, the

Table 1 Device performance of different hole injection layer based OLEDs.

Device ^{a)}	V	CE			PE			$\eta_{\text{ext}}^{\text{d)}$ (%)		
	[V] ^{b)}	[cd A ⁻¹] ^{c)}			[lm W ⁻¹] ^{c)}					
10%	4.17	39.5, 35.5, 26.4	32.7, 21.5, 10.5	21.5	19.0	14.0				
30%	4.16	42.0, 37.7, 25.1	40.1, 25.9, 10.9	22.5	19.8	13.0				
50%	3.82	40.0, 38.2, 25.5	39.0, 27.2, 13.8	20.8	19.6	12.9				
70%	3.76	38.5, 33.3, 23.3	34.5, 22.8, 11.8	20.3	17.4	12.0				
90%	3.74	37.5, 29.0, 18.7	37.4, 24.4, 12.1	20.2	15.4	9.8				
MoO ₃	3.69	36.0, 24.5, 14.2	36.1, 18.4, 7.9	19.4	14.5	9.3				
TS-CuPc	10.4	27.7, 25.1, 19.7	10.2, 6.9, 3.9	14.9	14.2	10.8				
ITO	4.26	25.0, 20.8, 13.1	23.1, 13.3, 5.9	13.1	11.6	8.5				

a) Devices with the same structure under different doping concentration of MoO₃ into TS-CuPc as an interfacial layer; b) Driving voltage at 1000 cd m⁻²; c) Efficiencies in the order of maximum, at 1000 cd m⁻² and at 5000 cd m⁻². d) External quantum efficiency (η_{ext}) in the order of maximum, at 1000 cd m⁻² and at 5000 cd m⁻².

device efficiency in TS-CuPc:MoO₃ based device is higher than that of the pristine MoO₃ based device at higher current densities, despite the MoO₃ based device showing the lowest driving voltage. We attributed it to the suppression of MoO_x diffusion by TS-CuPc in TS-CuPc:MoO₃ based devices.³⁶ Similar results were also obtained in green phosphorescent OLEDs (Supporting Information). In present work, the improved performance in MoO₃:TS-CuPc based devices was attributed to the reduced hole-injecting barrier height at the anode/doped HIL interface, and the reduced bulk resistivity in the doped HIL. What's more, the crystallization of TS-CuPc film could be alleviated by MoO₃ doping. Meanwhile, MoO₃ diffusion can be suppressed which is benefit to the device performance to some extent. It should be noted that PEDOT:PSS based device exhibited the highest driving voltage (the lowest current density at same voltage) while comparable current efficiency with the TS-CuPc:MoO₃ based one. Actually, many factors such as the luminance, the interface diffusion, the carrier recombination influence the device current efficiency besides the current density. The diffusion of MoO₃ and easy crystallization of TS-CuPc may lead to the not too high current efficiency in the MoO₃, TS-CuPc and TS-CuPc:MoO₃ based devices. And it was found that PEDOT:PSS based device presented the lowest power efficiency due to its highest driving voltage.

Mechanism of Enhanced Hole Injection

To further understand the enhanced injection with lowered driving voltage in TS-CuPc:MoO₃ based OLEDs, UPS evaluation of TS-CuPc:MoO₃ modified ITO samples with different doping ratios were performed. It was found that the work function of ITO is strongly influenced by the interfacial

modification of TS-CuPc:MoO₃. As shown in Fig. 6, pristine TS-CuPc film has the lowest work function which corresponds to the largest driving voltage in the device. With increasing the doping ratio of MoO₃, the secondary cutoffs of the UPS spectra shifted to the lower binding energy. This means that the work function of ITO could be improved by TS-CuPc:MoO₃ modification with large doping ratio.

Two hole-dominated devices (TS-CuPc and TS-CuPc:MoO₃ as

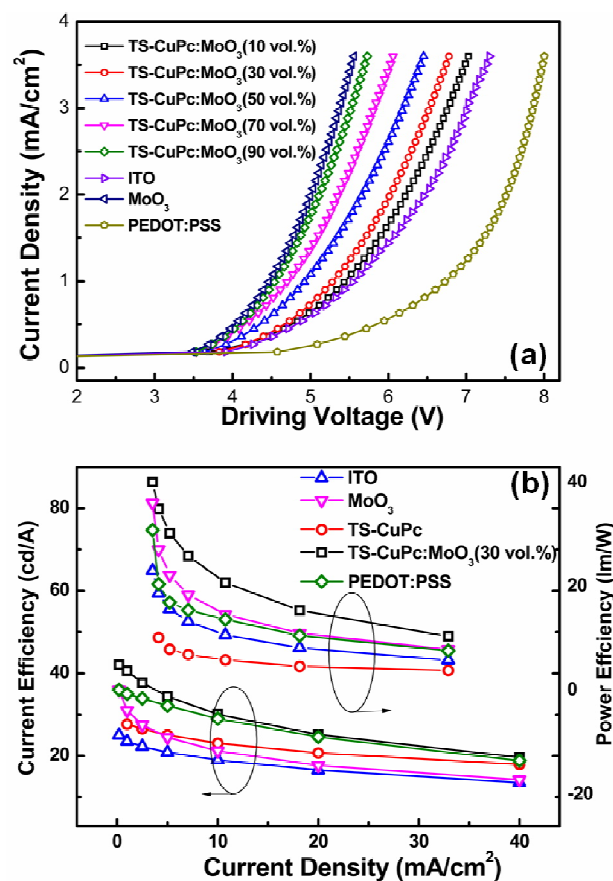


Fig. 5 (a) J - V characteristics of TS-CuPc:MoO₃ based OLEDs with different MoO₃ doping concentration. (b) Current efficiency and power efficiency characteristics in different hole interfacial layer based OLEDs.

interfacial layer, respectively) were fabricated. The electron blocking layer was removed to eliminate the potential effects of excessive interfaces and mobility-dependence for additional organic materials. The temperature-dependent J - V curves are shown in Fig. 7 (a). In TS-CuPc:MoO₃ based devices, the current density is four times higher than that in TS-CuPc based devices at the same voltage and identical temperature. The temperature-dependent J - V curves suggests that the hole injection was associated with a Schottky thermal emission mechanism.³⁷⁻³⁹ Although the Schottky thermionic emission model is not a realistic theory due to the complexity of the interface caused by material, chemical, structural and morphological factors,^{40,41} it provides a qualitative analysis and a trend of change injection process with different interfacial layers. The details of the

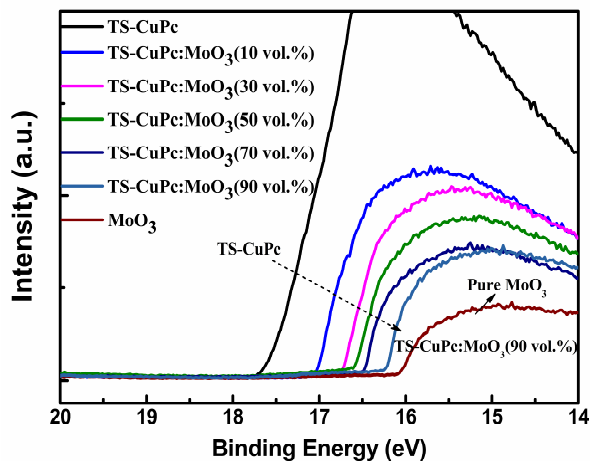


Figure 6 UPS spectra of TS-CuPc, MoO₃, TS-CuPc:MoO₃ with different MoO₃ doping ratio modified ITO samples.

barrier extrapolation according to the Schottky thermal emission model can be seen elsewhere.⁴² Fig. 7 (b) shows the relationship between $\ln J_0/T^2$ and $1/T$ in two hole-dominated devices. J_0 is current density at zero voltage by extrapolating straight lines to the ordinal point in the plot of $\ln J$ vs $V^{1/2}$. The slope of the extrapolated line gives the barrier height of 0.55 and 0.28 eV for TS-CuPc and TS-CuPc:MoO₃ based device, respectively. The injection current is proportional to $\exp(-q\phi_B/kT)$, where q is an electron charge, ϕ_B the injection barrier, k the Boltzmann constant, and T the temperature.

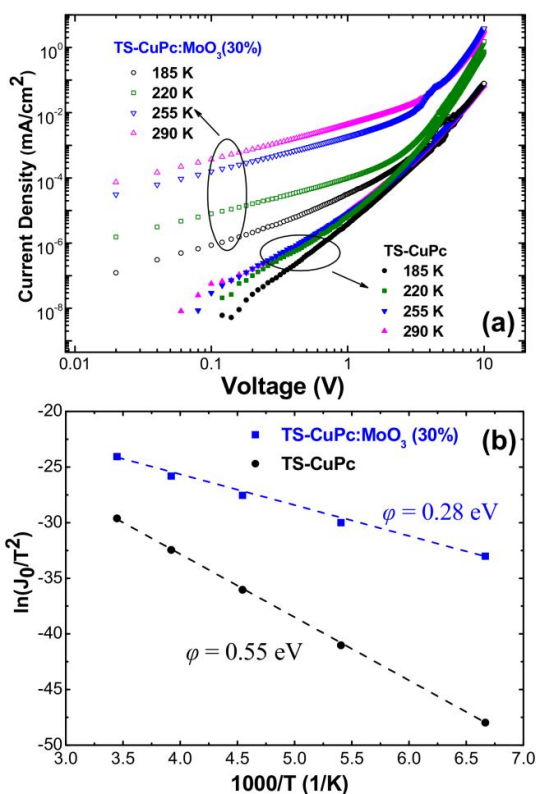


Fig. 7 (a) Temperature dependence of J - V characteristics in TS-CuPc and TS-CuPc:MoO₃ (30%) based hole-dominated devices; (b) The relationships between $\ln J_0/T^2$ and $1/T$, respectively. J_0 is current density at zero voltage by extrapolating straight lines to the ordinal point in the plot of $\ln J$ vs $V^{1/2}$.

Although the difference between the hole barrier heights in TS-CuPc and TS-CuPc:MoO₃ based devices is only 0.27 eV, it will cause a large difference in the current in two devices, which was consistent with the results as shown in Fig. 7 (a). Noticeably, the barrier height derived from the temperature-dependent J - V curves is not equal to the difference between the work function of ITO and the energy level of the adjacent organic layers, the difference just implies that some changes were taken place at the interfaces of anode/interfacial layer. In all, we attributed the enhanced hole injection and improved device performance to the efficient modifications of ITO by TS-CuPc:MoO₃. Charge transfer is realized in MoO₃ doped TS-CuPc based on an aqueous solution processing. TS-CuPc:MoO₃ composite film can act as an efficient hole injection and transport layer in OLEDs.

Conclusions

We have developed an efficient anode interfacial layer, MoO₃ doped TS-CuPc, in OLEDs through an environmentally-friendly and easy fabricating process. The absorption spectra and the XPS measurements revealed that charge transfer complex was formed in TS-CuPc:MoO₃ composite films based on their aqueous solutions. The TS-CuPc:MoO₃ interfacial layer based device exhibited lower driving voltage and higher efficiency than the pristine TS-CuPc based one. Enhanced hole injection was attributed to the decreased hole barrier at the ITO side, which agreed with the Schottky thermal emission evaluation. The efficient modifications of ITO by TS-CuPc:MoO₃ was further confirmed by the UPS measurements. The finding provides an effective anode interfacial layer for ITO modification, which has potential application in organic electronics especially the OLEDs.

Acknowledgements

We acknowledge financial support from the Natural Science Foundation of China (Nos. 61307036 and 61177016) and from the Natural Science Foundation of Jiangsu Province (No. BK20130288). This project is also funded by the Collaborative Innovation Center of Suzhou Nano Science and Technology, and by the Priority Academic Program Development of Jiangsu Higher Education Institutions (PAPD).

Notes and references

Jiangsu Key Laboratory for Carbon-Based Functional Materials & Devices, Institute of Functional Nano & Soft Materials (FUNSOM), and Collaborative Innovation Center of Suzhou Nano Science and Technology, Soochow University, Suzhou, Jiangsu 215123, China

Email: lsiao@suda.edu.cn; zkwang@suda.edu.cn

Electronic Supplementary Information (ESI) available: [AFM surface images and absorption spectra of MoO₃ doped TS-CuPc films with varied

- MoO₃ doping concentration; Device performance of TS-CuPc:MoO₃ based Ir(ppy)₂acac green OLEDs.] See DOI: 10.1039/b000000x/
- 1 C. W. Tang, S. A. VanSlyke, *Appl. Phys. Lett.*, 1987, 51, 913.
 - 2 M. G. Helander, Z. B. Wang, J. Qiu, M. T. Greiner, D. P. Puzzo, Z. W. Liu, Z. H. Lu, *Science*, 2011, 332, 944 .
 - 3 Z. K. Wang, Y. H. Lou, S. Naka, H. Okada, *Appl. Phys. Lett.*, 2011, 98, 063302.
 - 4 C. H. Gao, X. Z. Zhu, L. Zhang, D. Y. Zhou, Z. K. Wang, L. S. Liao, *Appl. Phys. Lett.*, 2013, 102, 153301.
 - 5 H. Lee, S. W. Cho, K. Han, P. E. Jeon, C. N. Whang, K. Jeong, K. Cho, Y. Yi, *Appl. Phys. Lett.*, 2008, 93, 043308.
 - 6 C. H. Gao, S. D. Cai, W. Gu, D. Y. Zhou, Z. K. Wang, L. S. Liao, *ACS Appl. Mater. Interfaces*, 2012, 4, 5211.
 - 7 C. C. Wu, C. I. Wu, J. C. Sturm, A. Kahn, *Appl. Phys. Lett.*, 1997, 70, 11.
 - 8 L. S. Hung, L. R. Zheng, M. G. Mason, *Appl. Phys. Lett.*, 2001, 78, 673.
 - 9 T. P. Nguyen, P. Le. Rendu, N. N. Dinh, M. Fourmigué, C. Mézière, *Synthetic Metals*, 2003, 138, 229.
 - 10 T. W. Lee, Y. Chung, O. Kwon, J. J. Park, *Adv. Funct. Mater.*, 2007, 17, 390.
 - 11 S. Y. Yu, J. H. Chang, P. S. Wang, C. I. Wu, Y. T. Tao, *Langmuir*, 2014, 30, 7369.
 - 12 Z. B. Wang, M. G. Helander, M. T. Greiner, J. Qiu, Z. H. Lu, *Phys. Rev. B.*, 2009, 80, 235325.
 - 13 T. Matsushima, Y. Kinoshita, H. Murata, *Appl. Phys. Lett.*, 2007, 91, 253504.
 - 14 X. L. Zhu, J. X. Sun, H. J. Peng, Z. G. Meng, M. Wong, H. S. Kwok, *Appl. Phys. Lett.*, 2005, 87, 153508.
 - 15 J. Meyer, T. Winkler, S. Hamwi, S. Schmale, H. H. Johannes, T. Weimann, P. Hinze, W. Kowalsky, T. Riedl, *Adv. Mater.*, 2008, 20, 3839.
 - 16 J. M. Caruge, J. E. Halpert, V. Bulovic, M. G. Bawendi, *Nano. Lett.*, 2006, 6, 2991.
 - 17 J. Liang, F. S. Zu, L. Ding, M. F. Xu, X. B. Shi, Z. K. Wang, L. S. Liao, *Appl. Phys. Exp.*, 2014, 7, 111601.
 - 18 X. B. Shi, M. F. Xu, D.Y. Zhou, Z. K. Wang, L. S. Liao, *Appl. Phys. Lett.*, 2013, 102, 233304.
 - 19 M. F. Xu, L. S. Cui, X. Z. Zhu, C. H. Gao, X. B. Shi, Z. M. Jin, Z. K. Wang, L. S. Liao, *Org. Electron.*, 2013, 14, 657.
 - 20 S. A. Van Slyke, C. H. Chen, C. W. Tang, *Appl. Phys. Lett.*, 1996, 69, 2160.
 - 21 H. Aziz, Z. D. Popovic, N. X. Hu, Ah-Mee Hor, G. Xu, *Science*, 1999, 283, 1900.
 - 22 R. Bechara, J. Petersen, V. Gernigon, P. Lévêque, T. Heiser, V. Toniazzo, D. Ruch, M. Michel, *Sol. Energy Mater. Sol. Cells*, 2012, 98, 482.
 - 23 M. Raïssi, L. Vignau, B. Ratier, *Org. Electron.*, 2014, 15, 913.
 - 24 Y. H. Lou, M. F. Xu, Z. K. Wang, S. Naka, H. Okada, L. S. Liao, *Appl. Phys. Lett.*, 2013, 102, 113305.
 - 25 Y. H. Lou, M. F. Xu, L. Zhang, Z. K. Wang, S. Naka, H. Okada, L. S. Liao, *Org. Electron.*, 2013, 14, 269.
 - 26 H. Ishii, K. Sugiyama, E. Ito, K. Seki, *Adv. Mater.*, 1999, 11, 972 .
 - 27 H. Vazquez, F. Flores, A. Kahn, *Org. Electron.*, 2007, 8, 241 .
 - 28 J. X. Tang, C. S. Lee, S. T. Lee, *J. Appl. Phys.*, 2007, 101, 064504 .
 - 29 T. W. Ng, M. F. Lo, M. K. Fung, W. J. Zhang, C. S. Lee, *Adv. Mater.*, 2014, 26, 5569.
 - 30 T. W. Ng, M. F. Lo, S. T. Lee, C. S. Lee, *Appl. Phys. Lett.*, 2012, 100, 113301 .
 - 31 T. W. Ng, M. F. Lo, S. T. Lee, C. S. Lee, *Org. Electron.*, 2012, 13, 1641 .
 - 32 L. Li, M. Guan, G. Cao, Y. Li, Y. Zeng, *Displays*, 2012, 33, 17.
 - 33 L. Li, M. Guan, G. Cao, Y. Li, Y. Zan, H. C. Huang, D. H. Yan, *Appl. Phys. Lett.*, 2005, 87, 093507 .
 - 34 X. Qiao, J. Chen, X. Li, D. Ma, *J. Appl. Phys.*, 2010, 107, 104505.
 - 35 L. Li, M. Guan, G. Cao, Y. Li, Y. Zeng, *Displays*, 2012, 33, 17.
 - 36 S. D. Cai, C. H. Gao, D. Y. Zhou, W. Gu, L. S. Liao, *ACS Appl. Mater. Interfaces*, 2012, 4, 312.
 - 37 Z. K. Wang, Y. H. Lou, S. Naka, Okada. H, *ACS Appl. Mater. Interfaces*, 2011, 3, 2496.
 - 38 H. L. Cheng, Y. S. Mai, W. Y. Chou, L. R. Chang, X. W. Liang, *Adv. Funct. Mater.*, 2007, 17, 3639.
 - 39 S. Wang, T. Minari, T. Miyadera, Y. Aoyagi, K. Tsukagoshi, *Appl. Phys. Lett.*, 2008, 93, 043311.
 - 40 J. C. Scott, *J. Vac. Sci. Technol. A*, 2003, 21, 521.
 - 41 Y. Shen, M. W. Klein, D. B. Jacobs, J. C. Scott, G. G. Malliaras, *Phys. Rev. Lett.*, 2001, 86, 3867.
 - 42 S. M. Sze, *Physics of Semiconductor Device*, 2nd ed., Wiley: New York, 1981, Chapter 5.

TOC

An efficient anode interfacial layer, MoO₃ doped TS-CuPc, in OLEDs through an environmentally-friendly fabricating process is developed.

